

# The application of *in utero* magnetic resonance imaging in the study of the metabolic and cardiovascular consequences of the developmental origins of health and disease

## Review

**Cite this article:** Giza SA, Sethi S, Smith LM, Empey M-EET, Morris LE, and McKenzie CA. (2021) The application of *in utero* magnetic resonance imaging in the study of the metabolic and cardiovascular consequences of the developmental origins of health and disease. *Journal of Developmental Origins of Health and Disease* **12**: 193–202. doi: [10.1017/S2040174420001154](https://doi.org/10.1017/S2040174420001154)

Received: 15 November 2019

Revised: 13 October 2020


Accepted: 23 October 2020

First published online: 14 December 2020

### Keywords:

Magnetic Resonance Imaging; Developmental origins of health and disease; pregnancy; fetal growth restriction; fetal development

**Address for correspondence:** Charles A. McKenzie, University of Western Ontario, Schulich School of Medicine and Dentistry, Department of Medical Biophysics, 70384 London, ON, Canada.  
Email: [cmcken@uwo.ca](mailto:cmcken@uwo.ca)

Stephanie A. Giza, Simran Sethi, Lauren M. Smith, Mary-ellen E. T. Empey, Lindsay E. Morris and Charles A. McKenzie 

University of Western Ontario, Schulich School of Medicine and Dentistry, Department of Medical Biophysics, 70384 London, ON, Canada

### Abstract

Observing fetal development *in utero* is vital to further the understanding of later-life diseases. Magnetic resonance imaging (MRI) offers a tool for obtaining a wealth of information about fetal growth, development, and programming not previously available using other methods. This review provides an overview of MRI techniques used to investigate the metabolic and cardiovascular consequences of the developmental origins of health and disease (DOHaD) hypothesis. These methods add to the understanding of the developing fetus by examining fetal growth and organ development, adipose tissue and body composition, fetal oximetry, placental microstructure, diffusion, perfusion, flow, and metabolism. MRI assessment of fetal growth, organ development, metabolism, and the amount of fetal adipose tissue could give early indicators of abnormal fetal development. Noninvasive fetal oximetry can accurately measure placental and fetal oxygenation, which improves current knowledge on placental function. Additionally, measuring deficiencies in the placenta's transport of nutrients and oxygen is critical for optimizing treatment. Overall, the detailed structural and functional information provided by MRI is valuable in guiding future investigations of DOHaD.

### Introduction

The developmental origin of health and disease (DOHaD) hypothesis suggests that the environment a fetus experiences *in utero* can impact that individual's health for the rest of their lives.<sup>1</sup> Barker observed that fetuses born very small had increased risk of cardiovascular disease as adults.<sup>2</sup> Maternal conditions such as obesity and diabetes can also affect the fetus's development, thus increasing the risk for later-life disease.<sup>3,4</sup> These examples demonstrate that individuals who have experienced negative *in utero* programming through maternal, placental, or fetal causes experience altered development that increases their risk for later-life health complications, many of which are metabolic in nature. Cardiovascular disease, obesity, and diabetes affect increasingly large portions of our population. Understanding the early-life programming that contributes to them may help reduce the burden of these health concerns for future generations. In this review, we will focus on the role of *in utero* magnetic resonance imaging (MRI) in the study of cardiovascular and metabolic consequences of the DOHaD relationship through fetal, placental, and maternal metabolic perturbations.

MRI was developed in the 1970s and is used to visualize the internal anatomy and assess the function of the human body.<sup>5</sup> In the 1980s, MRI was used to visualize the pregnant anatomy, offering a new modality to visualize the fetus and placenta.<sup>6</sup> A precautionary approach to safety limited the widespread adoption of MRI in pregnancy for many years. Current use of *in utero* MRI follows guidelines such as those set out by the American College of Radiology.<sup>7</sup> Recent safety studies have not found an increase in adverse outcomes during pregnancy and early childhood after *in utero* exposure to MRI if contrast agents are not used.<sup>8–12</sup> The major concerns related to MRI in pregnancy include heating of the fetus and placenta, acoustic noise damage to fetal and maternal hearing, and potential teratogenicity of magnetic fields. A more in-depth look into these concerns is presented in other review papers.<sup>13,14</sup>

The use of *in utero* MRI is increasing in both research and clinical practice as it offers many advantages over other imaging modalities.<sup>15</sup> MRI does not use ionizing radiation and is non-invasive, making it safe/ideal to use in studying a vulnerable population.<sup>10</sup> It is a modality with a large field-of-view, allowing visualization of the entire uterus in an image volume.<sup>16</sup> MRI provides excellent soft-tissue contrast and is multiparametric, enabling multiple contrast sources in a single examination.<sup>17,18</sup> Some of the MRI contrasts allow us to measure information about function in addition to structure, permitting assessment of oxygenation, metabolism, and

© The Author(s), 2020. Published by Cambridge University Press in association with the International Society for Developmental Origins of Health and Disease. This is an Open Access article, distributed under the terms of the Creative Commons Attribution-NonCommercial-ShareAlike licence (<http://creativecommons.org/licenses/by-nc-sa/4.0/>), which permits non-commercial re-use, distribution, and reproduction in any medium, provided the same Creative Commons licence is included and the original work is properly cited. The written permission of Cambridge University Press must be obtained for commercial re-use.

**Table 1.** Summary of different MRI techniques and their *in utero* application for studying the metabolic and cardiovascular consequences of DOHaD in humans

MRI technique	Placenta	Fetal body	Brain	Heart	Liver	Kidney	Lung	Spleen	Blood
Structural MRI	x	x	x	x	x	x	x	x	
Magnetization transfer	x								
Fat-only or chemical-shift encoded (CSE) MRI		x			x				
BOLD-fMRI	x		x		x			x	
Relaxometry	x		x		x				x
Diffusion-weighted imaging (DWI) and diffusion tensor imaging (DTI)	x								
Intravoxel incoherent motion (IVIM)	x								x
Arterial spin labeling (ASL)	x								x
Phase-contrast (PC) MRI				x					x
Magnetic resonance spectroscopy (MRS)	x		x						

perfusion, to name a few. Fast 2D imaging, such as single-shot spin-echo sequences, is routinely used to assess fetal and organ growth and development, especially in the brain. Diffusion imaging is frequently used to investigate pathological placental invasion<sup>19,20</sup> and has been used to measure lung maturity.<sup>21,22</sup> For more information on the basic MRI principles and essential topics related to fetal MRI, please refer to the recent review paper by Aertsen *et al.*<sup>23</sup>

In comparison, the use of positron-emission tomography (PET) and x-ray computed tomography (CT) in pregnant humans is uncommon due to the risks associated with ionizing radiation.<sup>24</sup> Nuclear medicine, including PET, is only performed on pregnant patients for diagnosis or therapy of life-threatening conditions.<sup>25</sup> While CT remains an essential tool in diagnostics regardless of pregnancy status, it is not commonly used in pregnancy research.<sup>26</sup> Neither of these modalities are used in prospective pregnancy research, as there is no clinical benefit to the patient to outweigh the risk of the ionizing radiation delivered through imaging. Ultrasound (US) is frequently used in pregnancy to assess structure and limited functional parameters.<sup>27</sup> Its relatively small field-of-view and typical 2D image presentation make visualization of the entire fetus difficult late in gestation.<sup>28</sup> US is also relatively insensitive to metabolism and oxygenation.

MRI does have limitations such as accessibility<sup>29</sup> and cost.<sup>30</sup> These barriers include health centers without access to advanced MRI techniques<sup>29</sup> or expertise to use them *in utero*. Furthermore, MRI is a relatively slow imaging technique and is therefore sensitive to maternal and fetal motion, the latter of which is random and unpredictable.<sup>31</sup> When investigating a developing fetus's small anatomy, partial volumes<sup>32,33</sup> and spatial resolution<sup>34</sup> can be limiting. Additionally, the physical configuration of the MRI system can limit the size of the patient that can be imaged, particularly in the late second and third trimesters. The increasing availability of larger bore MRI systems (70 cm bore) is alleviating this issue. Despite these limitations, *in utero* MRI provides us with a wealth of knowledge about fetal growth, development, and programming not previously available.

This review will describe different MRI techniques used to study the cardiovascular and metabolic consequences of DOHaD (Table 1). We will discuss the investigation of fetal growth and organ development, body composition and adipose tissue, oxygenation and oximetry, placental microstructure, diffusion, perfusion and flow, and metabolism using *in utero* MRI.

### Assessment of fetal growth and organ development

Fetal growth assessment is regularly used to identify fetuses growing insufficiently (fetal growth restriction, FGR) or excessively (macrosomia), both of which are associated with the later-life metabolic consequences of DOHaD. MRI can monitor fetal growth through volumetric measurements, which have been shown to be superior to US estimated fetal weight.<sup>35,36</sup> The excellent soft-tissue contrast provided by MRI also allows for the measurement of organ growth, including liver, kidneys, brain, lungs, heart, and placenta.<sup>37</sup> The assessment of differential organ growth is useful for identifying altered growth distributions such as asymmetric FGR. MRI sequence parameters are chosen to optimize the images for an organ or region of interest, and in some cases, specialized acquisitions and reconstructions are required. Most notably, the fetal heart requires dedicated MRI sequences due to the motion through the cardiac cycle. Recent fetal cardiac MRI techniques are discussed in a review by Macgowan *et al.*<sup>38</sup> These techniques could be applied to study cardiac remodeling in response to an adverse *in utero* environment as they offer excellent structural views of the fetal heart through the entire cardiac cycle. While the use of MRI for fetal organ assessment has been focused on understanding normal development or assessing congenital malformations, the knowledge gained will help future studies on the cardiovascular and metabolic consequences of the DOHaD hypothesis.

### Adipose tissue and body composition

The earliest reports of MR images in pregnancy include a description of visible fetal adipose tissue.<sup>6,39</sup> Today, the ability to image adipose tissue, including that of the fetus, has far surpassed these early descriptions. As a result, a review of current techniques to image adipose tissue shows how refined and varied these newer tools have become.<sup>40,41</sup>

Fetal adipose tissue can be used to assess developmental programming's effects because it reflects the fetus's energy deposition through pregnancy.<sup>42</sup> For instance, fetuses of mothers with diabetes have an increased risk of being born with macrosomia, often due to an increase in offspring adipose tissue.<sup>43</sup> Changes in adipose tissue may be an early indicator of an altered fetal metabolism that could result in the development of metabolic syndrome later in life. Through fetal MRI, Anblagan *et al.* observed that fetuses of

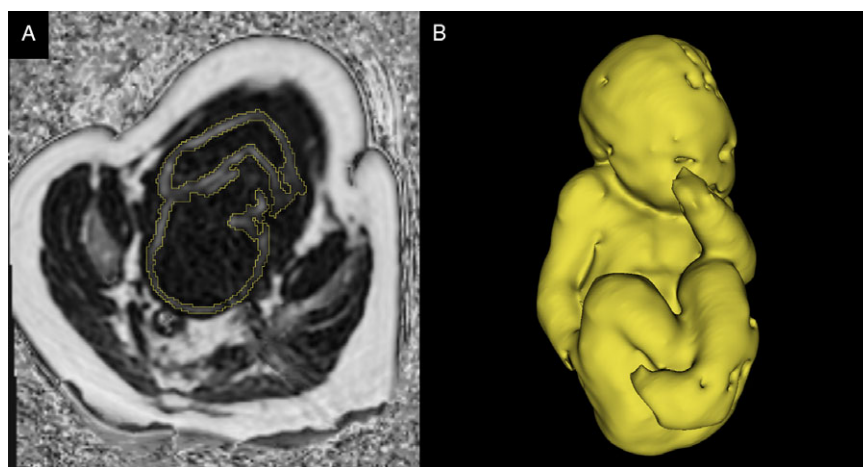


**Fig. 1.** (A) A single slice of 3D CSE-MRI image of third-trimester pregnancy. Bright pixels represent areas with high lipid content, and dark pixels represent areas of low lipid content. The segmentation of fetal adipose tissue is shown in yellow. (B) 3D rendering of segmented fetal adipose tissue. Image courtesy of the Pregnancy Research Group.

mothers with pre-existing diabetes had a greater adipose tissue volume than controls.<sup>44</sup> Using fat-only images at 34 weeks gestation, they found the total adipose tissue volume was increased and identified intra-abdominal adipose tissue more often in the fetuses of diabetic mothers.<sup>44</sup> Furthermore, using fat-only MR images, Berger-Kulemann *et al.* found that the fetuses of mothers with well-controlled diabetes did not have thicker subcutaneous adipose tissue than controls and attributed this to the strict control of the maternal glucose metabolism.<sup>45</sup> This finding suggests that careful control of the mother's metabolism may minimize the effects of metabolic diseases such as diabetes on the fetus's prenatal programming.

MRI is also capable of measuring the amount of lipid within a tissue using a method known as chemical shift encoded (CSE) MRI (see Fig. 1 for example images). CSE-MRI exploits the different resonant frequencies of lipids and water to create quantitative images of lipid or water content of tissues.<sup>46</sup> Giza *et al.* have used CSE-MRI in the fetus to show that fetal adipose tissue has an increasing proportion of lipid as the pregnancy progresses.<sup>47</sup> Furthermore, this technique has been applied to study a maternal high-fat diet's effect on fetal adipose tissue development in guinea pigs.<sup>48</sup> Sinclair *et al.* found that mothers exposed to a lifelong high-fat diet produced fetuses with increased lipid deposited in the adipose tissue and liver compared to those on a control diet.<sup>48</sup> These examples provide evidence that maternal metabolism can influence fetal metabolism to the extent that alterations in fetal adipose tissue development and lipid deposition are detectable with MRI, which may give early insight into the programming of the metabolic consequences of DOHaD.

Fetal motion is a significant obstacle for fetal MRI, including MRI of fetal adipose tissue. In the future, application of motion-resistant techniques, such as radial CSE-MRI,<sup>49</sup> to image the fetus should mitigate the problem of motion. CSE-MRI can also assess fatty acid saturation to determine the proportions of saturated, mono-unsaturated, and poly-unsaturated fatty acids in tissue.<sup>50</sup> This technique could give more insight into both maternal and fetal lipid metabolism.

After measuring fetal adipose tissue volume, fetal body composition can be determined by combining the adipose tissue measure with total fetal volume. Anblagan *et al.* used this idea to create a formula for estimating fetal weight using the different densities for fat mass and fat-free mass.<sup>44</sup> This technique could be extended to include a bone measurement using any MRI technique specialized for imaging bone<sup>51</sup> to determine the three main body composition compartments: bone mass, fat mass, and fat-free mass.

When applied to the fetus, this may allow researchers to study the effects of metabolism changes on any compartments of the developing body composition.

### Fetal and placental oximetry

One of the placenta's many functions is to provide the fetus with an adequate supply of oxygen.<sup>52</sup> However, if the placenta is impaired and unable to provide the fetus with adequate oxygen, the fetus is at risk for severe health conditions such as FGR.<sup>53,54</sup> Although techniques exist to assess the placenta's oxygen exchange, they are either invasive<sup>55</sup> or based on indirect measurements.<sup>56–58</sup> Fortunately, MRI provides noninvasive techniques that can be used to accurately measure changes in fetal and placental oxygenation.

MRI is sensitive to blood-oxygen content because of the difference in magnetic susceptibility between oxygenated and deoxygenated hemoglobin.<sup>59</sup> Two techniques that utilize this difference in magnetic properties are blood-oxygen-level-dependent (BOLD) MRI and vascular relaxometry.

BOLD imaging, often used in the brain, is the MR contrast mechanism used in functional MRI (fMRI) to visualize blood oxygenation changes related to neuronal activation.<sup>60</sup> Deoxyhemoglobin results in a decrease in the BOLD-fMRI signal, while oxyhemoglobin results in an increase,<sup>61</sup> allowing one to visualize the oxygen saturation change.

Numerous publications have focused on the use of BOLD-fMRI for assessing oxygenation in the placenta and other fetal organs in both animals and humans. It has been used to assess oxygen saturation change in the placenta and fetal organs in lambs under maternal hypoxia.<sup>62–64</sup> Sorensen *et al.* further investigated fetal liver oxygenation change in lambs, finding an oxygen saturation change in response to maternal hypoxia to be more pronounced in the right side of the fetal liver, which could be due to increased venous shunting.<sup>65</sup> Interestingly, unlike the placenta and other fetal organs, the fetal brain did not experience a change in the BOLD-fMRI signal when placed under hypoxic, normoxic, or hyperoxic conditions in fetal lambs.<sup>66</sup> This finding suggests a brain sparing mechanism<sup>67–69</sup> that was also observed in fetal mice.<sup>70</sup> In contrast, Wedegärtner *et al.* found a decrease in the BOLD-fMRI signal in fetal lamb brain, heart, and liver during maternal hypoxia, though the decrease in signal was significantly smaller in the brain compared to the other two organs.<sup>71</sup> BOLD-fMRI was also used to show a difference in response to maternal hyperoxygenation in growth-restricted fetal rats as they experienced a smaller increase in fetal tissue oxygenation compared to control fetal rats.<sup>72</sup>

In human studies, BOLD-fMRI has been used to investigate placental and fetal oxygenation primarily during maternal hyperoxia, a treatment implemented for increasing fetal oxygenation by providing oxygen to the mother.<sup>73,74</sup> During maternal hyperoxia, the oxygenation of the placenta and the fetal liver, fetal spleen, and fetal kidney was found to increase.<sup>75,76</sup> The brain sparing mechanism observed in fetal rats<sup>70</sup> has also been seen in humans as fetal brain oxygenation was not found to increase in response to maternal hyperoxia, in contrast to other fetal tissues.<sup>76,77</sup> Luo *et al.* further explored the utility of the BOLD-fMRI signal using placental time-to-plateau maps to assess placental oxygen transport in monozygotic twin pairs to encapsulate regional variations in placental function. This study found that in growth-restricted twins, the smaller twin needed more time to reach a hyperoxic steady state.<sup>78</sup> In summary, BOLD-fMRI has been used to successfully assess placental and tissue oximetry changes, which could provide information regarding the consequences of placental dysfunction in DOHaD.

BOLD-fMRI only provides relative oxygenation values rather than a quantitative value or quantitative change for blood volume or oxygen saturation.<sup>99</sup> Despite these limitations, it has the potential to be useful in many clinical applications. The next step for BOLD-fMRI would be assessing fetal response to maternal hyperoxia in cases of severely impaired placental function to better identify fetal nonresponsiveness, which is a predictor of adverse neonatal outcome.<sup>76</sup>

Vascular relaxometry is the measurement of the MR relaxation times ( $T_1$ ,  $T_2$ , and  $T_2^*$ ) of blood.<sup>79</sup> Due to the difference in deoxyhemoglobin and oxyhemoglobin's magnetic properties, the relaxation parameters of blood are sensitive to oxygen content.<sup>61</sup> By quantifying these relaxation times, fetal vascular properties, such as blood hematocrit and oxygen saturation, can be determined.<sup>80–83</sup>  $T_1$  and  $T_2$  relaxation times of fetal blood have been quantified as a function of blood hematocrit and oxygen saturation at 3.0 Tesla.<sup>84</sup> Human umbilical cord blood's relaxation times have also been quantified<sup>85</sup> and used to create models that estimate blood hematocrit and oxygen saturation.<sup>86</sup> Zhu *et al.* found the umbilical vein's  $T_2$  relaxation time to be a useful marker for assessing response to hypoxia in growth-restricted fetuses.<sup>87</sup> Another methodology that has been successful in assessing blood oxygenation is susceptibility-weighted imaging. The referenced studies have successfully used the principles of MRI susceptometry to evaluate fetal cerebral venous blood oxygenation saturation.<sup>88,89</sup> Furthermore, Yadav *et al.* showed a decrease in cerebral blood oxygenation with increasing gestation in second- and third-trimester fetuses,<sup>90</sup> most likely due to the marginal decrease in the umbilical venous blood oxygenation and increased metabolic demands of the fetus during the investigated gestational period.<sup>91,92</sup>

Tissue relaxometry has also been investigated, particularly in the placenta.<sup>93–96</sup> In the case of placental dysfunction,  $T_1$ ,  $T_2$ , and  $T_2^*$  were found to be lower than in gestational age (GA) matched normal placentae.<sup>93,94,96–99</sup> The decrease in these relaxation times is most likely due to changes in tissue oxygenation and morphology. These changes can be the result of the presence of problems like infarction or necrosis. Placental  $T_1$  has also been investigated in cases of maternal hyperoxia. In both normal and dysfunctional placentae, the hyperoxic  $T_1$  increased, representing an increase of  $PO_2$  in blood and tissue.<sup>99–101</sup> Furthermore, fetal liver  $T_2^*$  relaxation times were found to increase following maternal oxygenation.<sup>102</sup> Both vascular and placental relaxometry are sensitive to fetal oxygen change and can be used to assess oxygenation in cases of DOHaD.

Limitations with vascular relaxometry concern the biophysical models used to determine blood hematocrit and oxygen saturation. These limitations include the magnetic susceptibility differences between adult and fetal hemoglobin,<sup>88</sup> physiological variations between participants,<sup>85</sup> and bias from methemoglobin, which can decrease relaxation times.<sup>86</sup> Despite these limitations, vascular relaxometry can be useful in many clinical applications, and the next step can potentially be used to optimize the delivery timing of late-onset growth-restricted fetuses.<sup>87</sup>

### Placental microstructure

In addition to oxygenation, the microstructure of the placenta can be assessed using relaxometry. A negative correlation exists between placental  $T_1$  and GA, placental  $T_2$  and GA, and placental  $T_2^*$  and GA in normal placentae.<sup>93–96</sup> It has been speculated that the change in relaxation times is due to changes in morphology and function instead of changes in blood volume. Magnetization transfer ratio (MTR), which is the ratio of bound protons to total protons in tissue, is another quantitative measure used to investigate placental morphology. MTR reflects the non-vascular component of the placental volume relative to total placental volume. Ong *et al.* did not find placental MTR to vary significantly between GA groups or between normal pregnancies and those affected by FGR and pre-eclampsia.<sup>103</sup> These findings suggest that total placental volumes are maintained regardless of GA and the presence of FGR or pre-eclampsia. In short, both relaxometry and MTR can provide additional insight into placental composition, which could reflect placental adaptations to the *in utero* environment at a macromolecular level.

### Diffusion, perfusion, and flow

It can be challenging to identify a growth-restricted fetus *in utero*. There are still many cases of FGR that are left undiagnosed because current clinical methods for identification, such as umbilical artery Doppler ultrasound, fail to identify these fetuses, especially in obese women.<sup>104</sup> The ability to reliably and consistently identify FGR fetuses is critical for monitoring and early intervention.<sup>105</sup> Since the placenta provides nutrients and oxygen to the developing fetus via the maternal blood supply, any reduction in the placenta's blood flow and perfusion may result in FGR.<sup>106,107</sup> To improve clinical diagnostic capabilities for FGR and better understand placental function, several studies have used specialized MRI techniques to investigate normal and abnormal perfusion across placental compartments and assess microstructure and microvasculature. These techniques include diffusion-weighted imaging (DWI), diffusion tensor imaging (DTI), intravoxel incoherent motion (IVIM), arterial spin-labeling (ASL), and phase-contrast MRI (PC-MRI).

DWI and DTI are diffusion-based techniques that characterize water molecules' movement within tissues to investigate placental microstructure (see Fig. 2 for example images). DWI is sensitive to differences in the magnitude of water molecule diffusion ( $s/mm^2$ ), while DTI also accounts for the direction of water molecule diffusion.<sup>108</sup> Slatore *et al.* assessed diffusion in the healthy placenta and found differences across placental compartments, indicating distinct microvascular and tissue microstructure in the maternal and fetal sides of the placenta.<sup>109</sup> Diffusion MRI has been used to quantify the putative functional placental tissue (PFPT) volume, which is determined by high diffusion-weighted signal intensity in the placenta.<sup>105</sup> Diffusion parameters (diffusivity and fractional

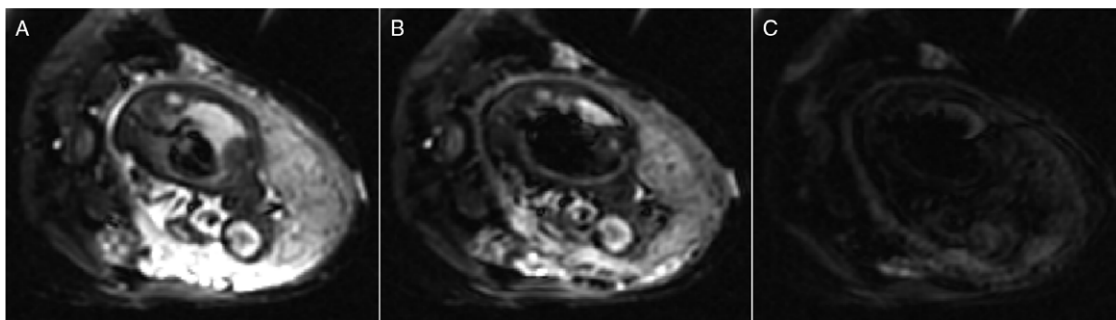


**Fig. 2.** Example of diffusion-weighted images of third-trimester pregnancy with different diffusion weightings [(A)  $b = 0$  s/mm<sup>2</sup>, (B)  $b = 35$  s/mm<sup>2</sup>, and (C)  $b = 750$  s/mm<sup>2</sup>]. It is possible to estimate diffusion and perfusion in tissues by performing a bi-exponential fit of MRI data with different diffusion weightings. Figure courtesy of C. Rockel and the Pregnancy Research Group.

anisotropy) are reduced in the PFPT of placental FGR compared to healthy controls, suggesting the development of the villous network is affected in placental FGR.<sup>105</sup> The volume of PFPT decreases significantly in placental FGR compared to healthy controls, while brain volume measured from diffusion images remains similar, indicating a brain sparing effect.<sup>110</sup> DWI and DTI may provide insight into placental villous development changes in examples of negative fetal programming, such as FGR.

While IVIM is a type of DWI, it differs in technique as IVIM utilizes additional parameters (perfusion fraction, pseudo-diffusion related to blood microcirculation) to characterize water molecule movement within each image voxel to provide a measure of perfusion and diffusion.<sup>111</sup> IVIM has poor sensitivity in low blood volume areas but performs well in high blood volume regions such as the placenta. It was shown to be a reproducible technique for measuring placental and fetal lung and liver perfusion, perfusion fraction, and diffusion.<sup>112</sup> Perfusion fraction measurements were less reliable, particularly in the kidneys and brain, due to small organ size and fetal motion.<sup>112</sup> It should be noted that the choice of MRI field strength (1.5 vs. 3.0 Tesla) affected the measured perfusion fraction of liver and lung, with higher perfusion fractions being measured at 3.0 Tesla.<sup>112</sup> These results highlight that IVIM is a difficult imaging technique to perform, particularly in the moving fetus's small organs. Despite these limitations, IVIM has been used to measure decreased perfusion fraction across the placenta in small for gestational age (SGA) compared to healthy controls in the second trimester.<sup>113</sup> IVIM measures of perfusion in healthy placentae showed a higher perfusion fraction in the outer (maternal) zone than the inner (fetal) zone.<sup>114</sup> The difference in perfusion is reduced in FGR compared to control pregnancies, as there is a reduction of placental perfusion fraction in the outer zone and slightly elevated perfusion fraction in the inner zone.<sup>114</sup> It should be noted that these studies were performed at single sites with relatively small numbers of patients, so larger multicenter studies are needed to confirm the utility of IVIM for fetoplacental assessment.

ASL magnetically labels the water molecules found in arterial blood to create an endogenous contrast agent to quantify perfusion (ml/min/g).<sup>111</sup> ASL has been used to investigate placental perfusion in healthy placentae of animals<sup>106</sup> and humans.<sup>113,115–117</sup> It has shown spatial heterogeneity in perfusion, which may be related to the cotyledons of the placenta.<sup>106,115–117</sup> Hutter *et al.* used ASL in combination with  $T2^*$  measurements to quantify placental perfusion and oxygenation in the healthy placenta.<sup>116</sup> ASL has also been used to identify SGA fetuses in the second trimester by measuring lower placental perfusion in SGA fetuses compared to

healthy controls.<sup>113</sup> Assessment of perfusion through IVIM or ASL in the placenta provides researchers and clinicians additional methods to probe placental function and adaptations.

PC-MRI is a technique used to measure flow on a larger scale than the perfusion measured by IVIM or ASL. PC-MRI is used to measure blood flow velocity (cm/s) as a function of time in either individual slices<sup>118</sup> or over a 3D volume.<sup>119</sup> From these data, it is possible to quantify the time-varying blood flow (ml/s) through vessels. PC-MRI has been used to determine ranges of blood flow through major fetal vessels in healthy pregnancies.<sup>118</sup> 3D PC-MRI (also known as 4D Flow) has been performed in pregnant large animal models to measure in- and out-flow of the uterus, umbilical cord, and fetal heart<sup>120</sup> and measure flow through major fetal vessels including the ductus venosus and ductus arteriosus.<sup>121</sup> Flow through the uterine arteries was also measured in human pregnancies, with velocity measurements agreeing with those obtained with Doppler US.<sup>122</sup> A strength of PC-MRI is the ability to assess blood flow in a 3D volume, which could allow assessment of placental and cardiovascular adaptations throughout gestation as a result of fetal programming.

A common limitation of diffusion and perfusion MRI is the lack of consensus in the choice of models used to fit placental diffusion data; however, Slator *et al.* have proposed an anisotropic IVIM model that explains human placental diffusion data better than the apparent diffusion coefficient, IVIM and DTI models.<sup>109</sup> There are a lack of data validating the diffusion and perfusion results against accepted clinical techniques, and some diffusion analysis methods can be adversely affected by placental location within the uterus.<sup>105,109</sup> The blood vessels that can be assessed with PC-MRI are limited by spatial resolution, making it difficult to perform in small animal models. In the future, studies may focus on developing techniques for clinical use, assessing placental microstructure in normal and abnormal placentae, and assessing of placental perfusion dynamics. Such developments would help understand placental adaptations to different DOHaD-related conditions such as maternal obesity, diabetes, and altered fetal growth.

### Metabolic MRI

Optimal fetoplacental metabolism is essential for the fetus's development *in utero*, and metabolic dysfunction is a possible cause of FGR.<sup>123</sup> In this section, we focus on the metabolic implications of FGR, which are relevant to DOHaD as growth restriction is known to impact health status later in life. A large focus of metabolic imaging is brain development; therefore, many of the spectroscopy

studies mentioned here investigate the developing brain's metabolic conditions *in utero*. MR techniques can provide direct measurements of metabolism *in vivo* and may be used to identify biomarkers useful to detect differences between normal and abnormal fetoplacental metabolism quantitatively.<sup>124</sup>

Magnetic resonance spectroscopy (MRS) provides data on metabolites *in vivo*, allowing for noninvasive measurements related to fetal or placental tissue's metabolic status. MRS measures the signal from hydrogen (<sup>1</sup>H) nuclei or other MR-sensitive nuclei, such as 31-phosphorus (<sup>31</sup>P). MRS is used to distinguish distinct molecules in a volume of interest based on their resonant frequencies and can be used to quantify the concentration of a metabolite by measuring the area under its spectral peak.<sup>124</sup> Successful fetoplacental MRS experiments have been demonstrated using clinical MRI scanners at field strengths of 1.5 and 3.0 Tesla.

The first study to demonstrate <sup>1</sup>H-MRS of the human placenta *in vivo* was published in 2012 by Denison *et al.*, specifically looking at choline, which is associated with a normal cell turnover rate in the developing fetal brain.<sup>125</sup> The study found a 60-fold reduction in the choline/lipid ratio in FGR fetuses' placentas, indicating placental failure and possible fetal hypoxia.<sup>125</sup> Glutamate and glutamine (Glx) are related to the production of nucleotides and amino sugars needed for cell proliferation and have also been studied via MRS in the human placenta. Macnaught *et al.* reported that FGR placentae were found to have a significantly lower Glx/choline ratio than healthy controls at the same GA,<sup>126</sup> demonstrating the prospect of Glx as a biomarker of placental function. <sup>31</sup>P-MRS has more recently been employed to study placental metabolism, with studies focusing on phosphodiester (PDE) and phosphomonoester (PME) metabolites important for cell membrane degradation and formation, respectively. This technique has been used to demonstrate an elevated PDE/PME ratio in the placenta for pregnancies with early-onset pre-eclampsia compared to healthy pregnancies,<sup>127</sup> as well as a case of abnormally high PDE signal from the placenta of a recently deceased fetus.<sup>128</sup>

<sup>1</sup>H-MRS has more commonly been used to study fetal brain metabolism, specifically targeting metabolites such as N-acetylaspartate (NAA), which is involved in neuronal metabolism, and lactate, which is related to hypoxia as a possible result of placental insufficiency.<sup>129</sup> Various <sup>1</sup>H-MRS fetal brain studies have reported differences between healthy and FGR fetuses, including elevated lactate found in brains of FGR fetuses<sup>127,129,130</sup> and reduced NAA/choline and NAA/creatine ratios in FGR fetuses.<sup>131–133</sup> Sanz-Cortes *et al.* included SGA fetuses in the study. They found that some SGA fetuses demonstrated reduced NAA/choline ratios similar to the FGR fetuses,<sup>132</sup> indicating that MRS may introduce a method of differentiating between metabolically healthy small fetuses and growth-restricted fetuses.

When studying complex systems like the fetus and placenta, it is useful to have spatial information to discern different metabolites' locations. Although non-proton MRI is useful for measuring different metabolites, it is challenging to perform due to low endogenous signal compared to <sup>1</sup>H. With the advancement of hyperpolarized (HP) MRI, it is possible to image non-proton molecules in a reasonable time frame by boosting the nuclear magnetic signal up to 10,000-fold.<sup>134</sup>

*In vivo* hyperpolarized MRI of the fetus or placenta is a very new field, and as such, there are only three animal studies in the literature to discuss. Friesen-Waldner *et al.* validated the technique of imaging injected hyperpolarized [<sup>1-<sup>13</sup>C</sup>]pyruvate and its downstream metabolites (lactate, alanine, and bicarbonate) *in utero* using 3D chemical shift imaging on a pregnant guinea pig model

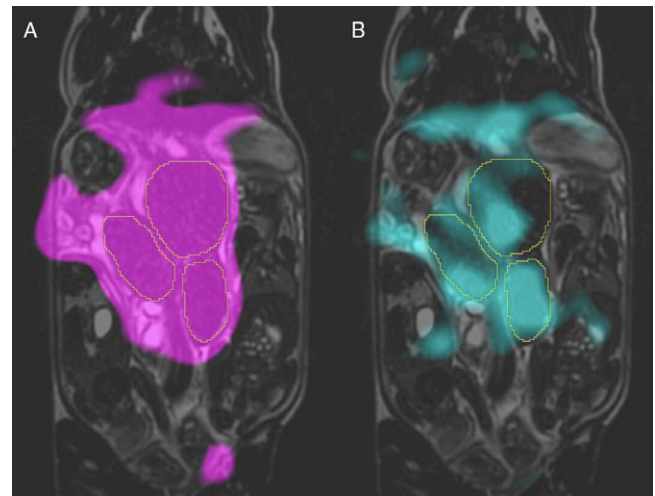


**Fig. 3.** Typical hyperpolarized <sup>13</sup>C metabolite images overlaid on coronal MRI of the same guinea pig at 22.5 s post-injection of [<sup>1-<sup>13</sup>C</sup>]pyruvate solution. Images of signal from two metabolites are shown here: pyruvate is shown in magenta (A) and lactate in cyan (B). The placentae are outlined in each image. Image courtesy of L. Smith, L. Friesen-Waldner, and T. Regnault.

(Fig. 3). This study reported pyruvate and lactate signal from all 30 healthy placentas and fetal livers.<sup>135</sup> A proof-of-concept paper by Markovic *et al.* focused on the use of the chinchilla as a model animal for fetoplacental research and used HP <sup>13</sup>C MRI to observe lactate and pyruvate in the placentae of four healthy pregnancies.<sup>136</sup> Lastly, Wang *et al.* investigated placental metabolism via HP <sup>13</sup>C MRI in a Wistar rat model of pre-eclampsia and observed differences in urea kinetics and pyruvate to lactate metabolism in the placentae of pre-eclamptic pregnancies compared to healthy pregnancies.<sup>137</sup> This study imaged three injected hyperpolarized substrates – [<sup>1-<sup>13</sup>C</sup>]pyruvate, <sup>13</sup>C-bicarbonate, and <sup>13</sup>C-urea – and reported observing urea, bicarbonate, pyruvate, lactate, and alanine in placentae, and urea in some fetal livers. It is important to note that HP <sup>13</sup>C MRI has been performed successfully in non-pregnant human subjects *in vivo*.<sup>137</sup> The validation of this technique in human patients combined with the success of fetoplacental imaging in multiple animal models suggests the obvious next step in this field is the translation to HP <sup>13</sup>C MRI studies of human pregnancy.

Both MRS and hyperpolarized MRI have challenges associated with them. An obvious challenge is fetoplacental motion, which may lead to MRS signal detection outside of intended voxels and artifacts in HP MRI images. Another challenge is the need for specific hardware, such as specialized RF coils for non-proton MRS and MRI. Limitations specific to MRS include long scan times that are not clinically translatable, difficulty performing small animal studies due to the low sensitivity resulting from the small fetus/placenta size, and limited spatial coverage. HP <sup>13</sup>C MRI limitations include the need for specialized equipment to hyperpolarize samples, limited resolution, and rapid signal decay that limits the temporal window for imaging post-injection.

## Conclusions

While we understand that the environment a fetus experiences *in utero* can alter its later-life health through developmental programming, the mechanisms supporting the DOHaD hypothesis remain unclear. Imaging may help answer some of the questions

regarding when and how this programming takes place. MRI is ideal for this task thanks to its ability to image different structures and function noninvasively during pregnancy.

Examining fetal growth and organ development allows for identifying under- or over-growth and deviations from normal organ development that may result from an adverse *in utero* environment. The ability to assess structural changes in adipose tissue and body composition can help determine if and when in gestation the programming is taking place, through alterations in lipid deposition resulting from altered nutrient availability. Measurement of placental and fetal oxygenation using MRI can provide insight into the placental tissue function and any fetal adaptations that compensate for deficiencies. Furthermore, MRI methods that assess diffusion and perfusion can provide additional insight into placental tissue structure and function. Finally, the ability to probe specific metabolites will help us understand the normal metabolic function of the fetus and placenta *in utero*. The information from the metabolites will also provide information about how the fetus and placenta can be altered in disease on a chemical level, making it one of the most powerful tools MRI has to offer the field of DOHaD.

This review of MRI used to study DOHaD has revealed a focus on FGR. However, we believe that MRI can help investigate other DOHaD-related metabolic or cardiovascular conditions, such as macrosomia, pre-eclampsia, maternal diabetes, and maternal obesity. It could also be a means of monitoring interventions aimed at reducing undesirable fetal programming throughout gestation.

Overall, MRI is a useful and diverse research tool for investigating the cardiovascular and metabolic consequences of DOHaD thanks to its excellent soft-tissue contrast and ability to quantify function in the fetus and placenta. The information it provides will help bridge the gap from the cellular mechanisms of programming to the clinical prevention of later-life disease.

**Acknowledgments.** The authors gratefully acknowledge support from Western University and Children's Health Research Institute/Children's Health Foundation.

**Financial support.** This work was supported by the Natural Sciences and Engineering Research Council of Canada (grant number RGPIN-2019-05708); the Canadian Institutes of Health Research (grant number 162308); and the National Institutes of Health (grant number 1U01HD087181-01).

**Conflicts of interest.** None.

## References

- Barker DJ. The fetal and infant origins of adult disease. *BMJ (Clinical research ed)*. 1990; 301(6761), 1111.
- Barker DJ. Fetal origins of coronary heart disease. *BMJ (Clinical research ed)*. 1995; 311(6998), 171–174.
- Oken E, Gillman MW. Fetal origins of obesity. *Obes Res*. 2003; 11(4), 496–506.
- Karter AJ, Rowell SE, Ackerson LM, *et al*. Excess maternal transmission of type 2 diabetes. The Northern California Kaiser permanente diabetes registry. *Diabetes Care*. 1999; 22(6), 938–943.
- Mansfield P, Maudsley AA. Medical imaging by NMR. *Br J Radiol*. 1977; 50(591), 188–194.
- Smith FW, Adam AH, Phillips WD. NMR imaging in pregnancy. *Lancet*. 1983; 1(1), 61–62.
- Radiology ACo. ACR-SPR Practice Parameter for the Safe and Optimal Performance of Fetal Magnetic Resonance Imaging (MRI). 2015. Available from: <https://www.acr.org/-/media/ACR/Files/Practice-Parameters/MR-Fetal.pdf>.
- Ray JG, Vermeulen MJ, Bharatha A, Montanera WJ, Park AL. Association between mri exposure during pregnancy and fetal and childhood outcomes. *JAMA*. 2016; 316(9), 952–961.
- Patenaude Y, Pugash D, Lim K, *et al*. The use of magnetic resonance imaging in the obstetric patient. *J Obstet Gynaecol Can: JOGC = Journal d'obstetrique et gynecologie du Canada: JOGC*. 2014; 36(4), 349–363.
- Stecco A, Saponaro A, Carriero A. Patient safety issues in magnetic resonance imaging: state of the art. *La Radiologia medica*. 2007; 112(4), 491–508.
- Jaffe TA, Miller CM, Merkle EM. Practice patterns in imaging of the pregnant patient with abdominal pain: a survey of academic centers. *AJR Am J Roentgenol*. 2007; 189(5), 1128–1134.
- Bulas D, Egloff A. Benefits and risks of MRI in pregnancy. *Semin Perinatol*. 2013; 37(5), 301–304.
- Lum M, Tsiouris AJ. MRI safety considerations during pregnancy. *Clin Imaging*. 2020; 62, 69–75.
- De Wilde JP, Rivers AW, Price DL. A review of the current use of magnetic resonance imaging in pregnancy and safety implications for the fetus. *Prog Biophys Mol Biol*. 2005; 87(2–3), 335–353.
- Glenn OA. MR imaging of the fetal brain. *Pediatr Radiol*. 2010; 40(1), 68–81.
- Levine D. Ultrasound versus magnetic resonance imaging in fetal evaluation. *Top Magn Reson Imaging: TMRI*. 2001; 12(1), 25–38.
- Frates MC, Kumar AJ, Benson CB, Ward VL, Tempany CM. Fetal anomalies: comparison of MR imaging and US for diagnosis. *Radiology*. 2004; 232(2), 398–404.
- Meyer-Wittkopf M, Cook A, McLennan A, Summers P, Sharland GK, Maxwell DJ. Evaluation of three-dimensional ultrasonography and magnetic resonance imaging in assessment of congenital heart anomalies in fetal cardiac specimens. *Ultrasound Obstet Gynecol Off J Int Soc Ultrasound Obstet Gynecol*. 1996; 8(5), 303–308.
- Dekan S, Linduska N, Kasprian G, Prayer D. MRI of the placenta - a short review. *Wien Med Wochenschr*. 2012; 162(9–10), 225–228.
- Aughwane R, Ingram E, Johnstone ED, Salomon LJ, David AL, Melbourne A. Placental MRI and its application to fetal intervention. *Prenatal Diagn*. 2020; 40(1), 38–48.
- Moore RJ, Strachan B, Tyler DJ, Baker PN, Gowland PA. In vivo diffusion measurements as an indication of fetal lung maturation using echo planar imaging at 0.5T. *Magn Reson Med*. 2001; 45(2), 247–253.
- Balassy C, Kasprian G, Brugger PC, *et al*. Diffusion-weighted MR imaging of the normal fetal lung. *Eur Radiol*. 2008; 18(4), 700–706.
- Aertsen M, Diogo MC, Dymarkowski S, Deprest J, Prayer D. Fetal MRI for dummies: what the fetal medicine specialist should know about acquisitions and sequences. *Prenatal Diagn*. 2020; 40(1), 6–17.
- Sreetharan S, Thome C, Tharmalingam S, *et al*. Ionizing radiation exposure during pregnancy: effects on postnatal development and life. *Radiat Res*. 2017; 187(6), 647–658.
- Stabin MG. Radiation dose and risks to fetus from nuclear medicine procedures. *Phys Med*. 2017; 43, 190–198.
- Goldberg-Stein S, Liu B, Hahn PF, Lee SI. Body CT during pregnancy: utilization trends, examination indications, and fetal radiation doses. *AJR Am J Roentgenol*. 2011; 196(1), 146–151.
- ACOG Practice Bulletin No. 101: Ultrasonography in pregnancy. *Obstet Gynecol*. 2009; 113(2 Pt 1), 451–461.
- Elliott ST. A user guide to extended field of view in ultrasonography. *Ultrasound*. 2006; 14(1), 55–28.
- Iron K, Przybysz R, Laupacis A. *Access to MRI in Ontario: Addressing the Information Gap*. Toronto: Institute for Clinical Evaluative Sciences, 2003.
- Sarracanie M, LaPierre CD, Salameh N, Waddington DEJ, Witzel T, Rosen MS. Low-cost high-performance MRI. *Sci Rep*. 2015; 5, 15177–15177.
- Quinn TM, Hubbard AM, Adzick NS. Prenatal magnetic resonance imaging enhances fetal diagnosis. *J Pediatr Surg*. 1998; 33(4), 553–558.
- Kneeland JB, Shimakawa A, Wehrli FW. Effect of intersection spacing on MR image contrast and study time. *Radiology*. 1986; 158(3), 819–822.
- Simmons A, Tofts PS, Barker GJ, Arridge SR. Sources of intensity nonuniformity in spin echo images at 1.5 T. *Magn Reson Med*. 1994; 32(1), 121–128.

34. Van Reeth E, Tham IWK, Tan CH, Poh CL. Super-resolution in magnetic resonance imaging: a review. *Concepts Magn Reson*. 2012; 40(6), 306–325.
35. Kadji C, Cannie MM, Resta S, et al. Magnetic resonance imaging for prenatal estimation of birthweight in pregnancy: review of available data, techniques, and future perspectives. *Am J Obstet Gynecol*. 2019; 220(5), 428–439.
36. Carlin A, Kadji C, Cannie MM, Resta S, Kang X, Jani JC. The use of magnetic resonance imaging in the prediction of birthweight. *Prenatal Diagn*. 2020; 40(1), 125–135.
37. Prayer D, Brugger PC. Investigation of normal organ development with fetal MRI. *Eur Radiol*. 2007; 17(10), 2458–2471.
38. Roy CW, van Amerom JFP, Marini D, Seed M, Macgowan CK. Fetal cardiac MRI: a review of technical advancements. *Top Magn Reson Imaging: TMRI*. 2019; 28(5), 235–244.
39. Smith FW, MacLennan F, Abramovich DR, MacGillivray I, Hutchison JMS. NMR imaging in human pregnancy: a preliminary study. *Magn Reson Med*. 1984; 2, 57–64.
40. Ma J. Dixon techniques for water and fat imaging. *J Magn Reson Imaging*. 2008; 28(3), 543–558.
41. Lemos T, Gallagher D. Current body composition measurement techniques. *Curr Opin Endocrinol, Diabetes, Obes*. 2017; 24(5), 310–314.
42. Ornoy A. Prenatal origin of obesity and their complications: gestational diabetes, maternal overweight and the paradoxical effects of fetal growth restriction and macrosomia. *Reprod Toxicol*. 2011; 32(2), 205–212.
43. Catalano PM, Thomas A, Huston-Presley L, Amini SB. Increased fetal adiposity: a very sensitive marker of abnormal in utero development. *Am J Obstet Gynecol*. 2003; 189(6), 1698–1704.
44. Anblagan D, Deshpande R, Jones NW, et al. Measurement of fetal fat in utero in normal and diabetic pregnancies using magnetic resonance imaging. *Ultrasound Obstet Gynecol Off J Int Soc Ultrasound Obstet Gynecol*. 2013; 42(3), 335–340.
45. Berger-Kulemann V, Brugger PC, Michael R, et al. Quantification of the subcutaneous fat layer with MRI in fetuses of healthy mothers with no underlying metabolic disease vs. fetuses of diabetic and obese mothers. *J Perinat Med*. 2012; 40(2), 179–184.
46. Reeder SB, Hu HH, Sirlin CB. Proton density fat-fraction: a standardized MR-based biomarker of tissue fat concentration. *J Magn Reson Imaging*. 2012; 36(5), 1011–1014.
47. Giza SA, Olmstead C, McCooeye DA, et al. Measuring fetal adipose tissue using 3D water-fat magnetic resonance imaging: a feasibility study. *J Matern-Fetal Neonat Med: Off J Eur Assoc Perinat Med Fed Asia and Oceania Perinat Soc Int Soc Perinat Obstet*. 2018; 1–7. doi: [10.1080/14767058.2018.1506438](https://doi.org/10.1080/14767058.2018.1506438).
48. Sinclair KJ, Friesen-Waldner LJ, McCurdy CM, et al. Quantification of fetal organ volume and fat deposition following in utero exposure to maternal Western Diet using MRI. *PLoS One*. 2018; 13(2), e0192900.
49. Benkert T, Feng L, Sodickson DK, Chandarana H, Block KT. Free-breathing volumetric fat/water separation by combining radial sampling, compressed sensing, and parallel imaging. *Magn Reson Med*. 2016; doi: [10.1002/mrm.26392](https://doi.org/10.1002/mrm.26392).
50. Bydder M, Girard O, Hamilton G. Mapping the double bonds in triglycerides. *Magn Reson Imaging*. 2011; 29(8), 1041–1046.
51. Werner H, Lopes Dos Santos JR, Ribeiro G, Belmonte SL, Daltro P, Araujo Junior E. Combination of ultrasound, magnetic resonance imaging and virtual reality technologies to generate immersive fetal 3D visualizations during pregnancy for fetal medicine studies. *Ultrasound Obstet Gynecol Off J Int Soc Ultrasound Obstet Gynecol*. 2016. doi: [10.1002/uog.17345](https://doi.org/10.1002/uog.17345).
52. Gude NM, Roberts CT, Kalionis B, King RG. Growth and function of the normal human placenta. *Thromb Res*. 2004; 114(5–6), 397–407.
53. Cetin I, Alvino G. Intrauterine growth restriction: implications for placental metabolism and transport. A review. *Placenta*. 2009; 30 (Suppl A), S77–S82.
54. Pardi G, Marconi AM, Cetin I. Placental-fetal interrelationship in IUGR fetuses—a review. *Placenta*. 2002; 23(Suppl A), S136–S141.
55. Liao C, Wei J, Li Q, Li L, Li J, Li D. Efficacy and safety of cordocentesis for prenatal diagnosis. *Int J Gynaecol Obstet Off Organ Int Fed Gynaecol Obstet*. 2006; 93(1), 13–17.
56. Madazli R, Somunkiran A, Calay Z, Ilvan S, Aksu MF. Histomorphology of the placenta and the placental bed of growth restricted fetuses and correlation with the Doppler velocimetry of the uterine and umbilical arteries. *Placenta*. 2003; 24(5), 510–516.
57. Rosen KG, Amer-Wahlin I, Luzietti R, Noren H. Fetal ECG waveform analysis. *Best Pract Res Clin Obstet Gynaecol*. 2004; 18(3), 485–514.
58. Baschat AA. Pathophysiology of fetal growth restriction: implications for diagnosis and surveillance. *Obstet Gynecol Surv*. 2004; 59(8), 617–627.
59. Pauling L, Coryell CD. The magnetic properties and structure of hemoglobin, oxyhemoglobin and carbonmonoxyhemoglobin. *Proc Natl Acad Sci USA*. 1936; 22(4), 210–216.
60. Logothetis NK. The neural basis of the blood-oxygen-level-dependent functional magnetic resonance imaging signal. *Philos Trans R Soc London, Ser B*. 2002; 357(1424), 1003–1037.
61. Ogawa S, Lee TM. Magnetic resonance imaging of blood vessels at high fields: in vivo and in vitro measurements and image simulation. *Magn Reson Med*. 1990; 16(1), 9–18.
62. Wedegartner U, Tchirikov M, Schafer S, et al. Functional MR imaging: comparison of BOLD signal intensity changes in fetal organs with fetal and maternal oxyhemoglobin saturation during hypoxia in sheep. *Radiology*. 2006; 238(3), 872–880.
63. Schoenagel BP, Yamamura J, Fischer R, et al. BOLD MRI in the brain of fetal sheep at 3T during experimental hypoxia. *J Magn Reson Imaging*. 2015; 41(1), 110–116.
64. Sorensen A, Holm D, Pedersen M, et al. Left-right difference in fetal liver oxygenation during hypoxia estimated by BOLD MRI in a fetal sheep model. *Ultrasound Obstet Gynecol Off J Int Soc Ultrasound Obstet Gynecol*. 2011; 38(6), 665–672.
65. Tchirikov M, Schroder HJ, Hecher K. Ductus venosus shunting in the fetal venous circulation: regulatory mechanisms, diagnostic methods and medical importance. *Ultrasound Obstet Gynecol Off J Int Soc Ultrasound Obstet Gynecol*. 2006; 27(4), 452–461.
66. Sorensen A, Pedersen M, Tietze A, Ottosen L, Duus L, Uldbjerg N. BOLD MRI in sheep fetuses: a non-invasive method for measuring changes in tissue oxygenation. *Ultrasound Obstet Gynecol Off J Int Soc Ultrasound Obstet Gynecol*. 2009; 34(6), 687–692.
67. Cohn HE, Sacks EJ, Heymann MA, Rudolph AM. Cardiovascular responses to hypoxemia and acidemia in fetal lambs. *Am J Obstet Gynecol*. 1974; 120(6), 817–824.
68. Gleason CA, Hamm C, Jones MD, Jr. Effect of acute hypoxemia on brain blood flow and oxygen metabolism in immature fetal sheep. *Am J Physiol*. 1990; 258(4 Pt 2), H1064–H1069.
69. Pearce W. Hypoxic regulation of the fetal cerebral circulation. *J Appl Physiol (Bethesda, Md : 1985)*. 2006; 100(2), 731–738.
70. Cahill LS, Zhou YQ, Seed M, Macgowan CK, Sled JG. Brain sparing in fetal mice: BOLD MRI and Doppler ultrasound show blood redistribution during hypoxia. *J Cereb Blood Flow Metab Off J Int Soc Cerebral Blood Flow Metab*. 2014; 34(6), 1082–1088.
71. Wedegartner U, Tchirikov M, Koch M, Adam G, Schröder H. Functional magnetic resonance imaging (fMRI) for fetal oxygenation during maternal hypoxia: initial results. *Rofo*. 2002; 174(6), 700–703.
72. Aimot-Macron S, Salomon LJ, Deloison B, et al. In vivo MRI assessment of placental and foetal oxygenation changes in a rat model of growth restriction using blood oxygen level-dependent (BOLD) magnetic resonance imaging. *Eur Radiol*. 2013; 23(5), 1335–1342.
73. Young DC, Popat R, Luther ER, Scott KE, Writer WD. Influence of maternal oxygen administration on the term fetus before labor. *Am J Obstet Gynecol*. 1980; 136(3), 321–324.
74. Willcourt RJ, King JC, Queenan JT. Maternal oxygenation administration and the fetal transcutaneous PO<sub>2</sub>. *Am J Obstet Gynecol*. 1983; 146(6), 714–715.
75. Sorensen A, Peters D, Frund E, Lingman G, Christiansen O, Uldbjerg N. Changes in human placental oxygenation during maternal hyperoxia estimated by blood oxygen level-dependent magnetic resonance imaging (BOLD MRI). *Ultrasound Obstet Gynecol Off J Int Soc Ultrasound Obstet Gynecol*. 2013; 42(3), 310–314.



76. Sorensen A, Peters D, Simonsen C, *et al.* Changes in human fetal oxygenation during maternal hyperoxia as estimated by BOLD MRI. *Prenatal Diagn.* 2013; 33(2), 141–145.
77. Huen I, Morris DM, Wright C, Sibley CP, Naish JH, Johnstone ED. Absence of PO<sub>2</sub> change in fetal brain despite PO<sub>2</sub> increase in placenta in response to maternal oxygen challenge. *BJOG: Int J Obstet Gynaecol.* 2014; 121(13), 1588–1594.
78. Luo J, Abaci Turk E, Bibbo C, *et al.* In vivo quantification of placental insufficiency by BOLD MRI: a human study. *Sci Rep.* 2017; 7(1), 3713.
79. Cistola DP, Robinson MD. Compact NMR relaxometry of human blood and blood components. *Trends Anal Chem TRAC.* 2016; 83(A), 53–64.
80. Thulborn KR, Waterton JC, Matthews PM, Radda GK. Oxygenation dependence of the transverse relaxation time of water protons in whole blood at high field. *Biochim Biophys Acta.* 1982; 714(2), 265–270.
81. Gomori JM, Grossman RI, Yu-IP C, Asakura T. NMR relaxation times of blood: dependence on field strength, oxidation state, and cell integrity. *J Comput Assisted Tomogr.* 1987; 11(4), 684–690.
82. Bryant RG, Marill K, Blackmore C, Francis C. Magnetic relaxation in blood and blood clots. *Magn Reson Med.* 1990; 13(1), 133–144.
83. Silvennoinen MJ, Kettunen MI, Kauppinen RA. Effects of hematocrit and oxygen saturation level on blood spin-lattice relaxation. *Magn Reson Med.* 2003; 49(3), 568–571.
84. Portnoy S, Milligan N, Seed M, Sled JG, Macgowan CK. Human umbilical cord blood relaxation times and susceptibility at 3 T. *Magn Reson Med.* 2018; 79(6), 3194–3206.
85. Portnoy S, Osmond M, Zhu MY, Seed M, Sled JG, Macgowan CK. Relaxation properties of human umbilical cord blood at 1.5 Tesla. *Magn Reson Med.* 2017; 77(4), 1678–1690.
86. Portnoy S, Seed M, Sled JG, Macgowan CK. Non-invasive evaluation of blood oxygen saturation and hematocrit from T1 and T2 relaxation times: In-vitro validation in fetal blood. *Magn Reson Med.* 2017; 78(6), 2352–2359.
87. Zhu MY, Milligan N, Keating S, *et al.* The hemodynamics of late-onset intrauterine growth restriction by MRI. *Am J Obstet Gynecol.* 2016; 214(3), 367 e361–367 e317.
88. Yadav BK, Buch S, Krishnamurthy U, *et al.* Quantitative susceptibility mapping in the human fetus to measure blood oxygenation in the superior sagittal sinus. *European radiology.* 2019; 29(4), 2017–2026.
89. Neelavalli J, Jella PK, Krishnamurthy U, *et al.* Measuring venous blood oxygenation in fetal brain using susceptibility-weighted imaging. *J Magn Reson Imaging: JMRI.* 2014; 39(4), 998–1006.
90. Yadav BK, Krishnamurthy U, Buch S, *et al.* Imaging putative foetal cerebral blood oxygenation using susceptibility weighted imaging (SWI). *European radiology.* 2018; 28(5), 1884–1890.
91. Schröter B, Chaoui R, Glatzel E, Bollmann R. [Normal value curves for intrauterine fetal blood gas and acid-base parameters in the 2nd and 3rd trimester]. *Gynakol Geburtshilfliche Rundsch.* 1997; 37(3), 130–135.
92. Burton GJ, Jauniaux E. Maternal vascularisation of the human placenta: does the embryo develop in a hypoxic environment? *Gynecol Obstet Fertil.* 2001; 29(7–8), 503–508.
93. Gowland PA, Freeman A, Issa B, *et al.* In vivo relaxation time measurements in the human placenta using echo planar imaging at 0.5 T. *Magn Reson Imaging.* 1998; 16(3), 241–247.
94. Duncan KR, Gowland P, Francis S, Moore R, Baker PN, Johnson IR. The investigation of placental relaxation and estimation of placental perfusion using echo-planar magnetic resonance imaging. *Placenta.* 1998; 19(7), 539–543.
95. Wright C, Morris DM, Baker PN, *et al.* Magnetic resonance imaging relaxation time measurements of the placenta at 1.5 T. *Placenta.* 2011; 32(12), 1010–1015.
96. Sinding M, Peters DA, Frokjaer JB, *et al.* Placental magnetic resonance imaging T2\* measurements in normal pregnancies and in those complicated by fetal growth restriction. *Ultrasound Obstet Gynecol Off J Int Soc Ultrasound Obstet Gynecol.* 2016; 47(6), 748–754.
97. Derwig I, Barker GJ, Poon L, *et al.* Association of placental T2 relaxation times and uterine artery Doppler ultrasound measures of placental blood flow. *Placenta.* 2013; 34(6), 474–479.
98. Sinding M, Peters DA, Poulsen SS, *et al.* Placental baseline conditions modulate the hyperoxic BOLD-MRI response. *Placenta.* 2018; 61, 17–23.
99. Ingram E, Morris D, Naish J, Myers J, Johnstone E. MR imaging measurements of altered placental oxygenation in pregnancies complicated by fetal growth restriction. *Radiology.* 2017; 285(3), 953–960.
100. Huen I, Morris DM, Wright C, *et al.* R1 and R2 \* changes in the human placenta in response to maternal oxygen challenge. *Magn Reson Med.* 2013; 70(5), 1427–1433.
101. Ingram E, Hawkins L, Morris DM, *et al.* R1 changes in the human placenta at 3 T in response to a maternal oxygen challenge protocol. *Placenta.* 2016; 39, 151–153.
102. Semple SI, Wallis F, Haggarty P, *et al.* The measurement of fetal liver T\*(\*) (2) in utero before and after maternal oxygen breathing: progress towards a non-invasive measurement of fetal oxygenation and placental function. *Magn Reson Imaging.* 2001; 19(7), 921–928.
103. Ong SS, Tyler DJ, Moore RJ, *et al.* Functional magnetic resonance imaging (magnetization transfer) and stereological analysis of human placentae in normal pregnancy and in pre-eclampsia and intrauterine growth restriction. *Placenta.* 2004; 25(5), 408–412.
104. Lauring JR, Gupta M, Kunselman AR, Repke JT, Pauli JM. Identification of small for gestational age by population-based and customized growth charts in newborns of obese and normal-weight primiparous women. *J Matern-Fetal Neonat Med Off J Eur Assoc Perinat Med Fed Asia Oceania Perinat Soc Int Soc Perinat Obstet.* 2016; 29(21), 3570–3574.
105. Javor D, Nasel C, Schweim T, Dekan S, Chalubinski K, Prayer D. In vivo assessment of putative functional placental tissue volume in placental intrauterine growth restriction (IUGR) in human fetuses using diffusion tensor magnetic resonance imaging. *Placenta.* 2013; 34(8), 676–680.
106. Ludwig KD, Fain SB, Nguyen SM, *et al.* Perfusion of the placenta assessed using arterial spin labeling and ferumoxytol dynamic contrast enhanced magnetic resonance imaging in the rhesus macaque. *Magn Reson Med.* 2019; 81(3), 1964–1978.
107. Chou FS, Yeh HW, Chen CY, *et al.* Exposure to placental insufficiency alters postnatal growth trajectory in extremely low birth weight infants. *J Dev Origins Health Dis.* 2019; 1–8. doi: [10.1017/s2040174419000564](https://doi.org/10.1017/s2040174419000564).
108. Meoded A, Poretti A, Mori S, Zhang J. Diffusion tensor imaging (DTI) ☆. In *Reference Module in Neuroscience and Biobehavioral Psychology*, 2017; pp. 1–10. Elsevier. doi: [10.1016/B978-0-12-809324-5.02472-X](https://doi.org/10.1016/B978-0-12-809324-5.02472-X).
109. Slator PJ, Hutter J, McCabe L, *et al.* Placenta microstructure and microcirculation imaging with diffusion MRI. *Magn Reson Med.* 2018; 80(2), 756–766.
110. Javor D, Nasel C, Dekan S, Gruber GM, Chalubinski K, Prayer D. Placental MRI shows preservation of brain volume in growth-restricted fetuses who suffer substantial reduction of putative functional placenta tissue (PFPT). *Eur J Radiol.* 2018; 108, 189–193.
111. Siauve N, Chalouhi GE, Deloison B, *et al.* Functional imaging of the human placenta with magnetic resonance. *Am J Obstet Gynecol.* 2015; 213(4 Suppl), S103–114.
112. Jakab A, Tuura R, Kottke R, Kellenberger CJ, Scheer I. Intra-voxel incoherent motion MRI of the living human foetus: technique and test-retest repeatability. *Eur Radiol Exp.* 2017; 1(1), 26.
113. Derwig I, Lythgoe DJ, Barker GJ, *et al.* Association of placental perfusion, as assessed by magnetic resonance imaging and uterine artery Doppler ultrasound, and its relationship to pregnancy outcome. *Placenta.* 2013; 34(10), 885–891.
114. Moore RJ, Strachan BK, Tyler DJ, *et al.* In utero perfusing fraction maps in normal and growth restricted pregnancy measured using IVIM echo-planar MRI. *Placenta.* 2000; 21(7), 726–732.
115. Shao X, Liu D, Martin T, *et al.* Measuring human placental blood flow with multidelay 3D GRASE pseudocontinuous arterial spin labeling at 3T. *J Magn Reson Imaging.* 2018; 47(6), 1667–1676.
116. Hutter J, Hartevelde AA, Jackson LH, *et al.* Perfusion and apparent oxygenation in the human placenta (PERFOX). *Magn Reson Med.* 2019. doi: [10.1002/mrm.27950](https://doi.org/10.1002/mrm.27950).
117. Gowland PA, Francis ST, Duncan KR, *et al.* In vivo perfusion measurements in the human placenta using echo planar imaging at 0.5 T. *Magn Reson Med.* 1998; 40(3), 467–473.

118. Prsa M, Sun L, van Amerom J, et al. Reference ranges of blood flow in the major vessels of the normal human fetal circulation at term by phase-contrast magnetic resonance imaging. *Circ Cardiovasc Imaging*. 2014; 7(4), 663–670.
119. Markl M, Frydrychowicz A, Kozerke S, Hope M, Wieben O. 4D flow MRI. *J Magn Reson Imaging*. 2012; 36(5), 1015–1036.
120. Macdonald JA, Corrado PA, Nguyen SM, et al. Uteroplacental and fetal 4D flow MRI in the pregnant rhesus macaque. *J Magn Reson Imaging*. 2019; 49(2), 534–545.
121. Schrauben EM, Saini BS, Darby JRT, et al. Fetal hemodynamics and cardiac streaming assessed by 4D flow cardiovascular magnetic resonance in fetal sheep. *J Cardiovasc Magn Reson*. 2019; 21(1), 8.
122. Hwuang E, Vidorreta M, Schwartz N, et al. Assessment of uterine artery geometry and hemodynamics in human pregnancy with 4d flow mri and its correlation with doppler ultrasound. *J Magn Reson Imaging*. 2019; 49(1), 59–68.
123. Sharma D, Shastri S, Sharma P. Intrauterine growth restriction: antenatal and postnatal aspects. *Clin Med Insights Pediatr*. 2016; 10, 67–83.
124. Arthurs OJ, Gallagher FA. Functional and molecular imaging with MRI: potential applications in paediatric radiology. *Pediatr Radiol*. 2011; 41(2), 185–198.
125. Denison FC, Semple SI, Stock SJ, Walker J, Marshall I, Norman JE. Novel use of proton magnetic resonance spectroscopy (1HMRS) to non-invasively assess placental metabolism. *PloS One*. 2012; 7(8), e42926.
126. Macnaught G, Gray C, Walker J, et al. (1)H MRS: a potential biomarker of in utero placental function. *NMR Biomed*. 2015; 28(10), 1275–1282.
127. Sohlberg S, Wikstrom AK, Olovsson M, et al. In vivo (3)(1)P-MR spectroscopy in normal pregnancy, early and late pre-eclampsia: a study of placental metabolism. *Placenta*. 2014; 35(5), 318–323.
128. Weindling AM, Griffiths RD, Garden AS, Martin PA, Edwards RH. Phosphorus metabolites in the human placenta estimated in vivo by magnetic resonance spectroscopy. *Arch Dis Child*. 1991; 66(7 Spec No), 780–782.
129. Charles-Edwards GD, Jan W, To M, Maxwell D, Keevil SF, Robinson R. Non-invasive detection and quantification of human foetal brain lactate in utero by magnetic resonance spectroscopy. *Prenatal Diagn*. 2010; 30(3), 260–266.
130. Cetin I, Barberis B, Brusati V, et al. Lactate detection in the brain of growth-restricted fetuses with magnetic resonance spectroscopy. *Am J Obstet Gynecol*. 2011; 205(4), 350.e351–357.
131. Azpurua H, Alvarado A, Mayobre F, Salom T, Copel JA, Guevara-Zuloaga F. Metabolic assessment of the brain using proton magnetic resonance spectroscopy in a growth-restricted human fetus: case report. *Am J Perinatol*. 2008; 25(5), 305–309.
132. Sanz-Cortes M, Simoes RV, Bargallo N, Masoller N, Figueras F, Gratacos E. Proton magnetic resonance spectroscopy assessment of fetal brain metabolism in late-onset ‘small for gestational age’ versus ‘intrauterine growth restriction’ fetuses. *Fetal Diagn Ther*. 2015; 37(2), 108–116.
133. Story L, Damodaram MS, Allsop JM, et al. Brain metabolism in fetal intrauterine growth restriction: a proton magnetic resonance spectroscopy study. *Am J Obstet Gynecol*. 2011; 205(5), 483.e481–488.
134. Ardenkjaer-Larsen JH, Fridlund B, Gram A, et al. Increase in signal-to-noise ratio of > 10,000 times in liquid-state NMR. *Proc. Natl. Acad. Sci. U. S. A.*. 2003; 100(18), 10158–10163.
135. Friesen-Waldner LJ, Sinclair KJ, Wade TP, et al. Hyperpolarized [1-(13)C]pyruvate MRI for non-invasive examination of placental metabolism and nutrient transport: a feasibility study in pregnant guinea pigs. *J Magn Reson Imaging*. 2016; 43(3), 750–755.
136. Markovic S, Fages A, Roussel T, et al. Placental physiology monitored by hyperpolarized dynamic (13)C magnetic resonance. *Proc. Natl. Acad. Sci. U. S. A.*. 2018; 115(10), E2429–e2436.
137. Wang ZJ, Ohliger MA, Larson PEZ, et al. Hyperpolarized (13)C MRI: state of the art and future directions. *Radiology*. 2019; 291(2), 273–284.